RESIDUAL STRESS/STRAIN ANALYSIS IN UO_2 SPENT FUEL BY SYNCHROTRON MICRO-BEAM X-RAY DIFFRACTION

G. KURI, M. MARTIN, J. BERTSCH

Paul Scherrer Institute, CH 5232 Villigen PSI, Switzerland

ABSTRACT

The macroscopic behavior of the irradiated UO_2 pellets is, to a great extent, determined by the UO_2 crystal lattice structure since the latter is associated with strain distributions within the irradiated crystallites and defines the defects population mechanisms responsible for the UO_2 grains subdivision at high damage levels. The aim of the study presented here is to evaluate the residual stress/strain present in irradiated UO_2 spent fuels within a single grain in the irradiated matrix and/or split grains domains. A sub-sample containing irradiated spent fuel particles (local burn up of about 45 MWd/kg) has been characterized using synchrotron based micro-beam X-ray diffraction (XRD). It is observed that UO_2 unit cell lattice parameter undergoes a significant expansion due to the effects of fission products dissolution and ingrowth of lattice defects in the irradiated matrix. The total strain in the irradiated sample is already above critical strain limit for UO_2 cracking. The consequence is the UO_2 grain-subdivision process or polygonization, also evidenced by synchrotron XRD. These results are presented and discussed.

1 Introduction

In order to extend burn-up of UO_2 fuel, one of the key issues for the technological step (i.e., fuel fabrication, intermediate storage, transport and reprocessing etc.) is to understand and ultimately control the fuel micro-structural changes. During the fission process a wide range of solid and gaseous fission product (FP) atoms are generated from the fissile uranium atoms in the fuel pellet. These new atoms impart energy and disturb the cation-cation and cation-anion network of the host UO_2 lattice. The formation of FPs together with other activation products leads to a doping of the UO_2 lattice depending on their solubility limit and chemical affinity in $UO_{2\pm x}$. As a consequence, the fission product atoms at a lower yield may be trapped at defect sites in the UO_2 lattice. At higher concentrations complex inter-metallic and other oxide precipitates involving solid FPs, Pu, U and O atoms can be formed which is controlled by the temperature, fission yield of elements and oxygen potential of the fuel. The gaseous FP atoms such as Kr and Xe, being practically insoluble in UO_2, always tend to agglomerate and form gas bubbles, move and accumulate at the grain boundaries detrimentally altering the in-service UO_2 microstructure at higher burn up.

Residual stress plays an important role in the microstructural details and associated structural properties that the irradiated UO_2 fuel exhibits. The macroscopic behavior of the irradiated pellets is, to a great extent, determined by the UO_2 crystal lattice structure [1-3] since the latter is associated with strain distributions within the irradiated crystallites, and defines the defects population mechanisms responsible for the UO_2 grains subdivision or fuel polygonization. The aim of this work is to show the potential of micro-beam XRD measurements to accurately characterize the local strain/stress state of grain specific UO_2 spent fuel materials. Let us mention that the present work is part of a broader systematic study [4] that aims at investigating the microstructural modifications by µXRD of irradiated UO_2 as a function of burn up and different operating conditions in the reactors.

2 Experimental

The specimens investigated were a commercial grade standard UO_2 fresh fuel pellet (4.8 wt.% enrichment with ^{235}U) in its final form, and materials from a spent fuel pellet of the same batch, irradiated with an average burnup of ~ 39 MWd/kg in the pellet. The analyzed fresh

fuel sample was a small UO_2 piece (about 1 mm^3). The irradiated fuel sample was prepared following a replica print method [5] for synchrotron experiment and µXRD measurements were performed on a sub-sample prepared from the irradiated UO_2 disc. In order to determine the precise local burn up of the fuel particles examined by X-rays, we have used the electron probe micro analysis (EPMA) data of fission product Neodymium (Nd) concentration. It is known that Nd is immobile in UO_2 and therefore can be used as an indicator of the radial burn-up distribution in a spent fuel pellet. In Fig. 1 the EPMA results for radial distribution of Neodymium in the fuel pellet is presented. The profile of elemental Nd fraction shows that concentration variation exists from the center to the outer periphery region in the spent fuel pellet. The circular mark in Fig. 1 is the radial location in the pellet from where tiny spent fuel particles were collected for synchrotron µXRD experiment. The burn up information obtained from the radial Nd profile at this location is about 45 MWd/kg.

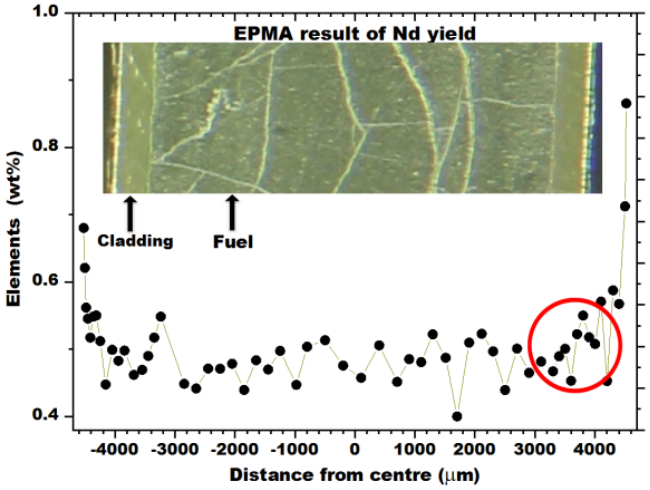

Fig. 1: the Neodymium concentration determined by EPMA in the fuel pellet. A sub-sample was prepared from a selected region (encircled in the figure) of the UO_2 pellet for µXRD measurements using synchrotron light. Inset shows the picture (longitudinal view) of the sample analyzed by EPMA.

Many details of the experimental arrangement for µXRD measurements on highly radioactive materials are described in a previous publication [5,6] and only a short description is provided here. We used the monochromatic X-ray (17200 eV) of a beamline X05L at the Swiss Light Source (SLS), Paul Scherrer Institute, Switzerland. A fixed-exit Si(111) double-crystal Bragg monochromator cooled with liquid nitrogen was used for the energy selection. The X-ray beam's focal size was 1 µm × 1 µm on the target. The diffracted light intensities were monitored with a charge-coupled-device (CCD) camera (photonic science, UK) in transmission mode by exposing the sample to X-rays. To prevent damaging the CCD, non-scattered X-rays were blocked with a 'beam-stop'. The range of diffraction is measured in 2θ, the angle of scattering between the incident beam and the diffracted X-rays. The relation of the CCD spot position to the Bragg angle was calibrated by recording Laue patterns from a reference corundum (α-Al_2O_3) powder specimen. Analysis of the XRD data involves FIT2D [7] and Match [8] programs. The diffraction peaks were indexed with those found in the literature and compared with international XRD database.

3 Results and discussion

With the use of micro-beam XRD technique, the analysis of UO_2 crystallinity on small areas of spent fuel particles has become possible. Careful analysis has been carried out on selected single spot Laue images and the corresponding diffraction line patterns in different regions within the fuel particles. The intensity distributions in µXRF maps are used to choose areas that minimized overlapping of different grain orientations and/or local thickness variation in the sample. This is necessary in selecting representative single spot diffraction spectra of interest originating apparently from identical domain volumes for a direct comparison of intensities or peaks identified by XRD and interpretation of data.

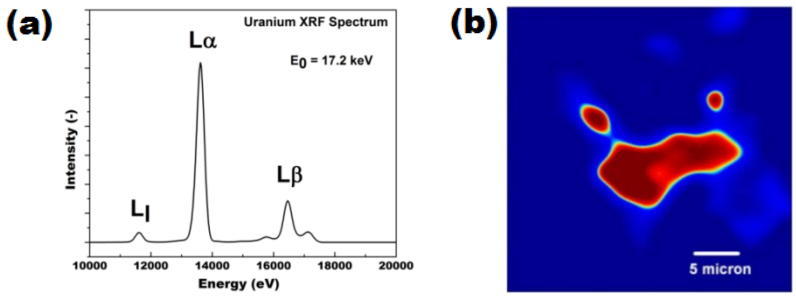

Fig. 2: (a) A typical example of μ-XRF spectrum, acquired with the excitation energy of 17200 eV from the UO_2 spent fuel sub-sample. The XRF signals of uranium L_l, Lα and Lβ lines are indicated in the figure. (b) High resolution μ-XRF color map of uranium intensity imaged from the sample.

The micro-XRF maps were obtained by scanning the surface of the UO_2 particles with a micro-focused X-ray beam while collecting the emitted fluorescence intensity from the specimen at grazing exit geometry. Figure 2 shows the uranium L-lines XRF spectrum and U-Lα fluorescence intensity map obtained from a 30 μm × 30 μm area of the sample. The larger irradiated fuel particle in the map has a size of about 15 μm × 8 μm, roughly comprising 2 to 3 adjacent UO_2 broken-grains, which roughly complies with the average grain size of ~ 10 μm for standard UO_2 microstructure. As seen in the image of Fig. 2b, uranium imaging provides a nearly homogeneous elemental distribution. However, it is important to note that although the μXRF technique could be successfully applied to detect those fuel particles, the lateral resolution is not high enough to distinguish UO_2 grains from other grains and grain-boundaries. The lateral resolution in the uranium map is furthermore limited by the penetration depth of the X-ray beam. Anyhow, the fuel particle illustrated in Fig. 2b is scanned though the X-ray beam in 1 μm steps. The probing region of the specimen in scanning μXRD was identified by the uranium μXRF map recorded.

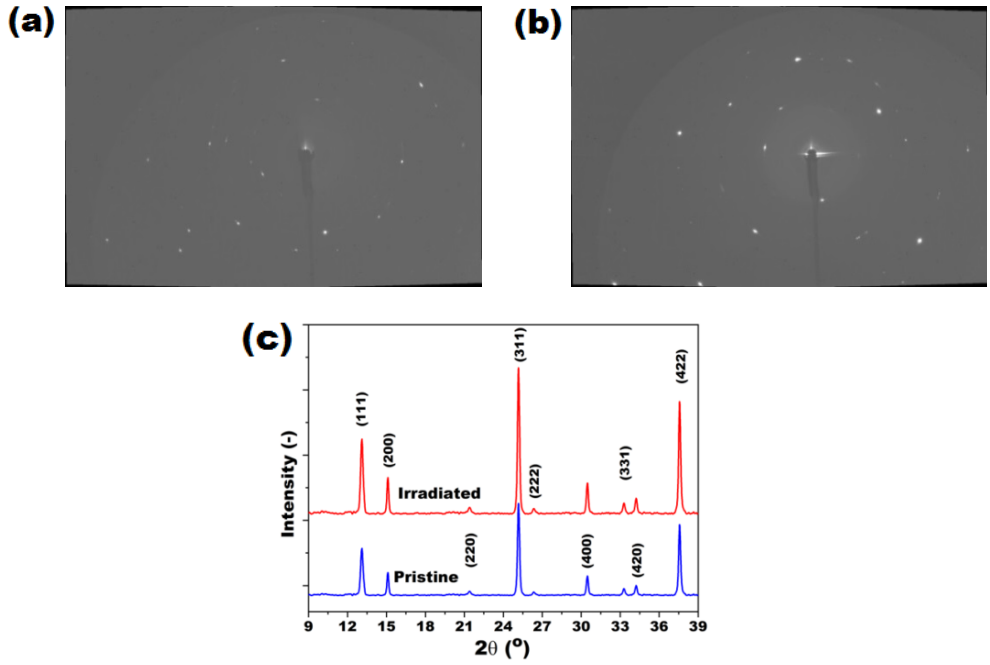

Fig. 3: Examples of the Laue patterns obtained from the two samples analyzed. (a) Fresh UO_2; (b) Irradiated UO_2. In (c), experimental μXRD intensity plots obtained after angular integration of a selected part of the 2D-diffraction diagrams of (a) and (b) are shown. See text for details.

Representative μXRD images collected from the pristine and irradiated UO_2 samples are shown in Fig. 3. It is evident that diffracted beams form arrays of spots lying on concentric circular curves. In general two distinct features are distinguished from the recorded diffraction patterns; fine circular spots and streaking of spots. Beside these two different components, a

couple of other weak reflections and features which varied substantially over the scanned area in irradiated samples, are observed but have not yet been fully analyzed. The pristine fuel sample exhibits strong single reflections (Fig. 3a) indicating the presence of large single crystallites. However, the irradiated material has undergone strong crystalline changes. The phenomenon of the Laue spots transforming to partial ring like structure implies that UO_2 grains are refined as a result of irradiation effects. Figure 3b demonstrates this process.

The 1D diffraction patterns of fresh and irradiated UO_2 are given in Fig. 3c. Several diffraction lines corresponding to (111), (200), (220), (311), (222), (400) and higher (*hkl*) patterns are observed from the UO_2 samples. The cubic lattice parameter of each sample is evaluated by analyzing the (422) reflection in detail using the XRDUA [9] computer program. This high-2θ diffraction peak (at about 37.5^o) is chosen to ensure higher sensitivity to the determination of UO_2 unit cell parameter. The peak positions and widths have been resolved by profile fitting and a Gaussian function is chosen as the X-ray diffraction peak profile in this study. Background intensity is subtracted before a peak fitting. The residuals peak-fitting procedure provides an interactive peak-fitting process until a minimum residual between fitted and experimental curve is reached. Then, the 2θ position of (422) reflex is determined from the fitting process. The XRD pattern of the (422) line for irradiated UO_2 has a peak position shift and broadened linewidth when compared to those of pristine fuel sample. From the measured angular position of the diffraction line the unit cell UO_2 lattice parameter, *a*, is estimated to be 5.472 Å and 5.483 Å (lattice constant error ±0.002 Å) for the pristine and irradiated samples, respectively. This result highlights the expansion of UO_2 lattice in spent fuel, which can be attributed to the effects of fission products dissolution and ingrowth of lattice defects in the irradiated matrix. Theoretical analyses of lattice parameter evolution, however, show that the components of the lattice parameters that are derived for the dissolved FPs largely balance out and only a small contribution to the lattice parameter remains. A detailed theoretical treatment of the effect of fission products incorporation in predicting their site occupancy in $UO_{2\pm x}$ [10] which generate information required for the anticipated change of irradiated UO_2 lattice spacing due to only successive doping with soluble FPs, and analysis of prevailing defect structure in irradiated UO_2 matrix are not be given here, but the overall effect should be a lattice expansion for an intermediate burn up of about 45 MWd/kg.

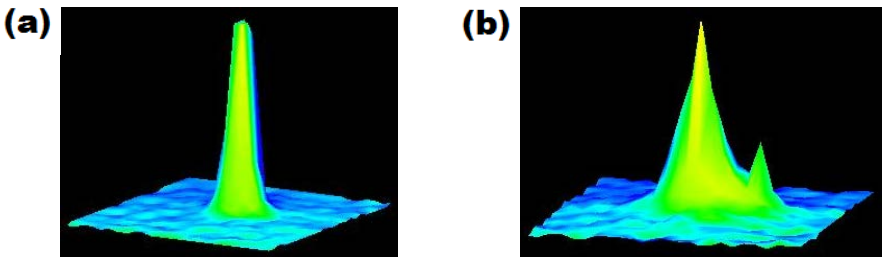

4: Laue spot patterns and comparison of intensity distribution for the (311) diffraction peak: (a) pristine UO_2 and (b) irradiated UO_2. Transverse streaking and splitting of Laue spots can be observed in the XRD data of spent fuel sample.

Interesting features has been identified for the irradiated UO_2 sample where modification of the Laue spot shapes is observed along transverse direction. These Laue patterns exhibit clear and strong streaking that are distinctly different from the other spots representing reflections of the same (*hkl)* plane families. However, no transverse streaking could be identified in spot patterns from fresh UO_2 sample. An example of Laue spot evolution and intensity distribution over a limited azimuth range of (311) diffraction line is shown in Fig. 4. Within the complete data set in scanning μXRD of irradiated UO_2 particles, slight transverse curvatures, uniform as well as non-uniform streaking in spots, and splitting of spots describing subdivision of original UO_2 grains, are also observed in some cases. These data have not yet been analyzed in detail, and are therefore not presented. In this work, we have

focused on the strain/stress analyses and estimated the elastic strain energy density that accumulates in irradiated UO_2 sample. For this reason, we have analyzed some of those selected single Laue spots and the corresponding diffraction line patterns where any significant level of Laue pattern streaking and/or change in Laue spot shape in transverse direction can be excluded.

The deviation from ideal crystallinity in irradiated UO_2 lattice has led to a broadening of the diffraction peaks and shifts the Bragg peak 2θ positions accordingly. As the crystallite size and lattice strain affect the Bragg peak in different ways, the strain-induced broadening in irradiated UO_2 and the strain factors, both uniform and non-uniform strain, have been calculated from the experimental XRD data and using the mathematical formalism reported in Refs. [3,11]. Strain values obtained are the uniform crystal strain (ε_c) of 0.22%, the non-uniform strain (ε_{nu}) or microstrain of 0.30%, and a total strain [$\varepsilon_{total}=\varepsilon_c+\sqrt{(2/\pi)}.\varepsilon_{nu}$] of about 0.45% for the analyzed UO_2 spent fuel sample having a burnup of 45 MWd/kg. The magnitude of this mentioned lattice strain is already above critical strain limit for UO_2 deformation [6], providing sufficient evidence in favor of the polygonization scenario as illustrated in Fig. 4. The results of this study are relevant for a better understanding of damage and weakening of the microstructure locally in irradiated UO_2, also in view of high burn up structure formation at a later stage, and the increasing tendency to fuel fragmentation under temperature excursions.

4 Conclusions

The method of non-destructive micro-beam Laue diffraction using synchrotron light has been used to determine atomic scale structural alteration of UO_2 crystallites in discharged spent fuel of a burn up of approximately 45 MWd/kg. From the XRD data, it is determined that the irradiated sample has larger lattice parameter than the pristine UO_2, presumably due to the presence of fission products and radiation defects in the irradiated matrix. Relevant here is the total strain and the first steps of UO_2 polygonization evident from micro-beam X-ray work, which otherwise may not be observed from commonly employed other microscopy techniques. A future paper will describe the comprehensive analysis of the results of the microstructural modifications by μXRD of irradiated UO_2 as a function of burn up and different operating conditions in the reactors.

Acknowledgements

We sincerely thank the team of micro-XAS beam line at PSI-SLS for their help for carrying out experimental work. We gratefully acknowledge the Hot-Laboratory technical-staff at PSI for preparing the radioactive specimens.

5 References

[1] J. H. Davies, F. T. Ewart, J. Nucl. Mater. 41 (1971) 143.

[2] J. Spino, D. Papaioannou, J. Nucl. Mater. 281 (2000) 146.

[3] M. Amaya, J. Nakamura, T. Fuketa, J. Nucl. Sci. Tech. 45 (2008) 244.

[4] M. Chollet, C. Cozzo, V. A. Samson, J. Bertsch, J. Nucl. Mater. (2018) [To be published].

[5] C. Degueldre, M. Martin, G. Kuri, D. Grolimund, C. Borca, J. Nucl. Mater. 416 (2011) 142.

[6] C. Mieszczynski, G. Kuri, C. Degueldre, M. Martin, J. Bertsch, C. N. Borca, D. Grolimund, Ch. Delafoy, E. Simoni, J. Nucl. Mater. 444 (2014) 274; and references therein.

[7] A. P. Hammersley, S. Svensson, A. Thompson, Nucl. Instrum. Meth. Phys. Res., A346 (1994) 312.

[8] http://www.crystalimpact.com/match.

[9] W. De Nolf, K. Janssens, Surf. Interface Anal. 42 (2010) 411.

[10] R. W. Grimes, C. R. A. Catlow, Phil. Trans.: Phys. Sci. Eng. 335 (1991) 609.

[11] M. Amaya, J. Nakamura, T. Fuketa, Y. Kosaka, J. Nucl. Mater. 396 (2010) 32.